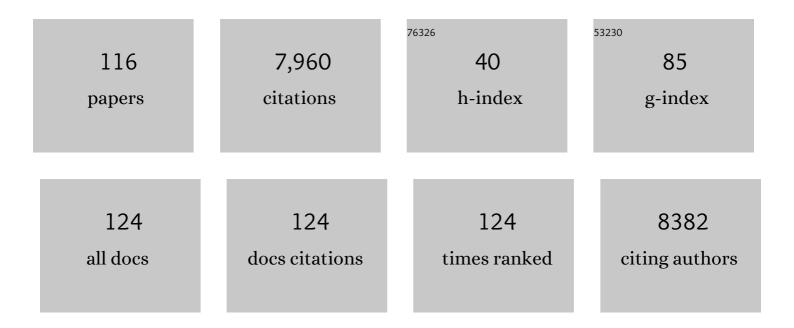
Robert F Dannals

List of Publications by Year in descending order

Source: https://exaly.com/author-pdf/5021066/publications.pdf Version: 2024-02-01



#	Article	IF	CITATIONS
1	Neural basis of alertness and cognitive performance impairments during sleepiness. I. Effects of 24 h of sleep deprivation on waking human regional brain activity. Journal of Sleep Research, 2000, 9, 335-352.	3.2	914
2	Chemogenetics revealed: DREADD occupancy and activation via converted clozapine. Science, 2017, 357, 503-507.	12.6	813
3	Selective hypometabolism in the inferior frontal lobe in depressed patients with Parkinson's disease. Annals of Neurology, 1990, 28, 57-64.	5.3	400
4	Positron emission tomographic imaging of the dopamine transporter with ¹¹ Câ€WIN 35,428 reveals marked declines in mild Parkinson's disease. Annals of Neurology, 1993, 34, 423-431.	5.3	321
5	Mu-opiate receptors measured by positron emission tomography are increased in temporal lobe epilepsy. Annals of Neurology, 1988, 23, 231-237.	5.3	253
6	Increased mu opioid receptor binding detected by PET in cocaine–dependent men is associated with cocaine craving. Nature Medicine, 1996, 2, 1225-1229.	30.7	250
7	Mania after brain injury: Neuroradiological and metabolic findings. Annals of Neurology, 1990, 27, 652-659.	5.3	238
8	Imaging Opiate Receptors in the Human Brain by Positron Tomography. Journal of Computer Assisted Tomography, 1985, 9, 231-236.	0.9	237
9	PSMA-Based [18F]DCFPyL PET/CT Is Superior to Conventional Imaging for Lesion Detection in Patients with Metastatic Prostate Cancer. Molecular Imaging and Biology, 2016, 18, 411-419.	2.6	202
10	Column-switching HPLC for the analysis of plasma in PET imaging studies. Nuclear Medicine and Biology, 2000, 27, 627-630.	0.6	191
11	Quantification of mu and non-mu opiate receptors in temporal lobe epilepsy using positron emission tomography. Annals of Neurology, 1991, 30, 3-11.	5.3	189
12	¹⁸ F-DCFBC PET/CT for PSMA-Based Detection and Characterization of Primary Prostate Cancer. Journal of Nuclear Medicine, 2015, 56, 1003-1010.	5.0	180
13	Positron emission tomography imaging of serotonin transporters in the human brain using [11C](+)McN5652. Synapse, 1995, 20, 37-43.	1.2	161
14	In vivo detection of short- and long-term MDMA neurotoxicity?a positron emission tomography study in the living baboon brain. Synapse, 1998, 29, 183-192.	1.2	141
15	PET imaging of microglia by targeting macrophage colony-stimulating factor 1 receptor (CSF1R). Proceedings of the National Academy of Sciences of the United States of America, 2019, 116, 1686-1691.	7.1	140
16	Radiosynthesis of an opiate receptor binding radiotracer: [11C]carfentanil. The International Journal of Applied Radiation and Isotopes, 1985, 36, 303-306.	0.7	136
17	Imaging of Glial Cell Activation and White Matter Integrity in Brains of Active and Recently Retired National Football League Players. JAMA Neurology, 2017, 74, 67.	9.0	134
18	Comparison of Prostate-Specific Membrane Antigen–Based ¹⁸ F-DCFBC PET/CT to Conventional Imaging Modalities for Detection of Hormone-NaÃīve and Castration-Resistant Metastatic Prostate Cancer. Journal of Nuclear Medicine, 2016, 57, 46-53.	5.0	111

#	Article	IF	CITATIONS
19	Imaging of ?- and ?-opioid receptors in temporal lobe epilepsy by positron emission tomography. Annals of Neurology, 1997, 41, 358-367.	5.3	107
20	Peptide-Based ⁶⁸ Ga-PET Radiotracer for Imaging PD-L1 Expression in Cancer. Molecular Pharmaceutics, 2018, 15, 3946-3952.	4.6	102
21	Localization of serotonin 5-HT2 receptors in living human brain by positron emission tomography using N1-([11C]-methyl)-2-BR-LSD. Synapse, 1987, 1, 393-398.	1.2	94
22	Quantification of Human Opiate Receptor Concentration and Affinity Using High and Low Specific Activity [¹¹ C]Diprenorphine and Positron Emission Tomography. Journal of Cerebral Blood Flow and Metabolism, 1991, 11, 204-219.	4.3	94
23	Neural basis of alertness and cognitive performance impairments during sleepiness II. Effects of 48 and 72 h of sleep deprivation on waking human regional brain activity. Thalamus & Related Systems, 2003, 2, 199.	0.5	91
24	Dynamic imaging in patients with tuberculosis reveals heterogeneous drug exposures in pulmonary lesions. Nature Medicine, 2020, 26, 529-534.	30.7	87
25	In vivo imaging of dopamine reuptake sites in the primate brain using single photon emission computed tomography (SPECT) and iodine-123 labeled RTI-55. Synapse, 1992, 10, 169-172.	1.2	85
26	Cannabinoid CB2 Receptors in a Mouse Model of AÎ ² Amyloidosis: Immunohistochemical Analysis and Suitability as a PET Biomarker of Neuroinflammation. PLoS ONE, 2015, 10, e0129618.	2.5	83
27	Characterization of 3 Novel Tau Radiopharmaceuticals, ¹¹ C-RO-963, ¹¹ C-RO-643, and ¹⁸ F-RO-948, in Healthy Controls and in Alzheimer Subjects. Journal of Nuclear Medicine, 2018, 59, 1869-1876.	5.0	81
28	Noninvasive ¹¹ C-rifampin positron emission tomography reveals drug biodistribution in tuberculous meningitis. Science Translational Medicine, 2018, 10, .	12.4	73
29	Preclinical Evaluation of ¹⁸ F-RO6958948, ¹¹ C-RO6931643, and ¹¹ C-RO6924963 as Novel PET Radiotracers for Imaging Tau Aggregates in Alzheimer Disease. Journal of Nuclear Medicine, 2018, 59, 675-681.	5.0	71
30	[123/1251]RTI-55, an in vivo label for the serotonin transporter. Synapse, 1992, 11, 134-139.	1.2	70
31	Imaging of ? opioid receptors in human brain by N1?- ([11C]methyl)naltrindole and PET. , 1996, 24, 19-28.		69
32	Synthesis of a radiotracer for studying nicotinic acetylcholine receptors: (+/â^`)-exo-2-(2-[18F]fluoro-5-pyridyl)-7-azabicyclo[2.2.1]heptane. Journal of Labelled Compounds and Radiopharmaceuticals, 1996, 38, 355-365.	1.0	67
33	Imaging Muscarinic Cholinergic Receptors in Human Brain in vivo with SPECT, [1231]4-lododexetimide, and [1231]4-lodolevetimide. Journal of Cerebral Blood Flow and Metabolism, 1992, 12, 562-570.	4.3	60
34	An improved synthesis of the radiolabeled prostate-specific membrane antigen inhibitor, [¹⁸ F]DCFPyL. Journal of Labelled Compounds and Radiopharmaceuticals, 2016, 59, 439-450.	1.0	59
35	[125/123I]IPH: A radioiodinated analog of epibatidine for in vivo studies of nicotinic acetylcholine receptors. , 1997, 26, 392-399.		52
36	Radiosynthesis of 3-[18F]fluoropropyl and 4-[18F]fluorobenzyl triarylphosphonium ions. Journal of Labelled Compounds and Radiopharmaceuticals, 2004, 47, 469-476.	1.0	52

#	Article	IF	CITATIONS
37	Doses of GBR12909 that suppress cocaine self-administration in non-human primates substantially occupy dopamine transporters as measured by [11C] WIN35,428 PET scans. , 1999, 32, 44-50.		50
38	GBR12909 attenuates amphetamine-induced striatal dopamine release as measured by [11C]raclopride continuous infusion PET scans. Synapse, 1999, 33, 268-273.	1.2	50
39	Imaging <i>Enterobacterales</i> infections in patients using pathogen-specific positron emission tomography. Science Translational Medicine, 2021, 13, .	12.4	49
40	Cerebral Glucose Utilization in Polysubstance Abuse. Neuropsychopharmacology, 1995, 13, 21-31.	5.4	48
41	Determination of [¹¹ C]Rifampin Pharmacokinetics within Mycobacterium tuberculosis-Infected Mice by Using Dynamic Positron Emission Tomography Bioimaging. Antimicrobial Agents and Chemotherapy, 2015, 59, 5768-5774.	3.2	47
42	Development of a High-Affinity PET Radioligand for Imaging Cannabinoid Subtype 2 Receptor. Journal of Medicinal Chemistry, 2016, 59, 7840-7855.	6.4	47
43	Imaging glial activation in patients with post-treatment Lyme disease symptoms: a pilot study using [11C]DPA-713 PET. Journal of Neuroinflammation, 2018, 15, 346.	7.2	46
44	Cerebral Glucose Utilization Is Reduced in Second Test Session. Journal of Cerebral Blood Flow and Metabolism, 1997, 17, 704-712.	4.3	43
45	Nicotine induced up-regulation of nicotinic receptors in CD-1 mice demonstrated with an in vivo radiotracer: Gender differences. Synapse, 1998, 30, 116-118.	1.2	40
46	Synthesis of carbon-11 labeled diprenorphine: A radioligand for positron emission tomographic studies of opiate receptors. Tetrahedron Letters, 1987, 28, 4015-4018.	1.4	38
47	In vivo studies of opiate receptors. Annals of Neurology, 1984, 15, 85-92.	5.3	37
48	Multiparametric Molecular Imaging Provides Mechanistic Insights into Sympathetic Innervation Impairment in the Viable Infarct Border Zone. Journal of Nuclear Medicine, 2015, 56, 457-463.	5.0	37
49	Use of Positron Emission Tomography to Study AT1 Receptor Regulation In Vivo. Journal of the American Society of Nephrology: JASN, 2001, 12, 1350-1358.	6.1	37
50	Decreased hippocampal muscarinic cholinergic receptor binding measured by1231-iododexetimide and single-photon emission computed tomography in epilepsy. Annals of Neurology, 1993, 34, 235-238.	5.3	35
51	[11C]-GR89696, a potent kappa opiate receptor radioligand; in vivo binding of the R and S enantiomers. Nuclear Medicine and Biology, 2002, 29, 47-53.	0.6	34
52	Development of imaging agents for the dopamine transporter. Medicinal Research Reviews, 1995, 15, 419-444.	10.5	33
53	1-(2,4-dichlorophenyl)-4-cyano-5-(4-[11C]methoxyphenyl)-N-(piperidin-1-yl)-1H-pyrazole-3-carboxamide ([11C]JHU75528) and 1-(2-bromophenyl)-4-cyano-5-(4-[11C]methoxyphenyl)-N-(piperidin-1-yl)-1H-pyrazole-3-carboxamide ([11C]IHU75575) as potential radioligands for PET imaging of cerebral cannabinoid receptor. Journal of	1.0	32
54	[11C]-methyl 4-[(3,4-dichlorophenyl)acetyl]-3-[(1-pyrrolidinyl)methyl]-1-piperazinecarboxylate ([11C]CR89696): synthesis and in vivo binding to kappa opiate receptors. Nuclear Medicine and Biology, 1999, 26, 737-741.	0.6	28

#	Article	IF	CITATIONS
55	¹¹ C-MCG: Synthesis, Uptake Selectivity, and Primate PET of a Probe for Glutamate Carboxypeptidase II (NAALADase). Molecular Imaging, 2002, 1, 153535002002021.	1.4	27
56	The distribution of the alpha7 nicotinic acetylcholine receptor in healthy aging: An in vivo positron emission tomography study with [18F]ASEM. NeuroImage, 2018, 165, 118-124.	4.2	27
57	Characterization of [11C]RO5013853, a novel PET tracer for the glycine transporter type 1 (GlyT1) in humans. Neurolmage, 2013, 75, 282-290.	4.2	26
58	Buprenorphine Reduces Cerebral Glucose Metabolism in Polydrug Abusers. Neuropsychopharmacology, 1994, 10, 157-170.	5.4	25
59	Neuroimaging of translocator protein in patients with systemic lupus erythematosus: a pilot study using [¹¹ C]DPA-713 positron emission tomography. Lupus, 2017, 26, 170-178.	1.6	25
60	Feasibility Evaluation of Myocardial Cannabinoid Type 1 Receptor ImagingÂinÂObesity. JACC: Cardiovascular Imaging, 2018, 11, 320-332.	5.3	24
61	Mechanistic Insights into Sympathetic Neuronal Regeneration. Circulation: Cardiovascular Imaging, 2015, 8, e003507.	2.6	23
62	Synthesis and quality control of [¹⁸ F]T807 for tau PET imaging. Journal of Labelled Compounds and Radiopharmaceuticals, 2016, 59, 411-415.	1.0	23
63	Synthesis of a mGluR5 antagonist using [11C]copper(I) cyanide. Journal of Labelled Compounds and Radiopharmaceuticals, 2006, 49, 829-834.	1.0	22
64	High Availability of the α7-Nicotinic Acetylcholine Receptor in Brains of Individuals with Mild Cognitive Impairment: A Pilot Study Using ¹⁸ F-ASEM PET. Journal of Nuclear Medicine, 2020, 61, 423-426.	5.0	22
65	Synthesis of N1â€2-([11C]methyl)naltrindole ([11C]MeNTI): A radioligand for positron emission tomographic studies of delta opioid receptors. Journal of Labelled Compounds and Radiopharmaceuticals, 1995, 36, 137-145.	1.0	21
66	Synthesis of a radioiodinated analog of epibatidine: (A±)-exo-2-(2-iodo-5-pyridyl)-7-azabicyclo[2.2.1]heptane for in vitro and in vivo studies of nicotinic acetylcholine receptors. Journal of Labelled Compounds and Radiopharmaceuticals, 1997, 39, 39-48.	1.0	21
67	Doseâ€dependent, saturable occupancy of the metabotropic glutamate subtype 5 receptor by fenobam as measured with [¹¹ C]ABP688 PET imaging. Synapse, 2014, 68, 565-573.	1.2	21
68	Facile synthesis of [11C]buprenorphine for positron emission tomographic studies of opioid receptors. International Journal of Radiation Applications and Instrumentation Part A, Applied Radiation and Isotopes, 1990, 41, 745-752.	0.5	19
69	Synthesis of [11C]gefitinib for imaging epidermal growth factor receptor tyrosine kinase with positron emission tomography. Journal of Labelled Compounds and Radiopharmaceuticals, 2006, 49, 883-888.	1.0	19
70	18F-FNDP for PET Imaging of Soluble Epoxide Hydrolase. Journal of Nuclear Medicine, 2016, 57, 1817-1822.	5.0	19
71	Positron emission tomography radioligands for the opioid system. Journal of Labelled Compounds and Radiopharmaceuticals, 2013, 56, 187-195.	1.0	18
72	PET-measured longitudinal flow gradient correlates with invasive fractional flow reserve in CAD patients. European Heart Journal Cardiovascular Imaging, 2016, 18, jew116.	1.2	18

#	Article	IF	CITATIONS
73	Noncompartmental and compartmental modeling of the kinetics of carbon-11 labeled pyrilamine in the human brain. Synapse, 1993, 15, 263-275.	1.2	17
74	Radiosynthesis of [11C]paclitaxel. Journal of Labelled Compounds and Radiopharmaceuticals, 2002, 45, 471-477.	1.0	17
75	Dissociative Changes in the B _{max} and K _D of Dopamine D ₂ /D ₃ Receptors with Aging Observed in Functional Subdivisions of the Striatum: A Revisit with an Improved Data Analysis Method. Journal of Nuclear Medicine, 2012, 53, 805-812.	5.0	17
76	Synthesis of [18F] SR144385: a selective radioligand for positron emission tomographic studies of brain cannabinoid receptors. Journal of Labelled Compounds and Radiopharmaceuticals, 1999, 42, 589-596.	1.0	16
77	Synthesis and initialin vitro characterization of 6-[18F]fluoro-3-(2(S)-azetidinylmethoxy)pyridine, a high-affinity radioligand for central nicotinic acetylcholine receptors. Journal of Labelled Compounds and Radiopharmaceuticals, 2000, 43, 413-423.	1.0	16
78	Pre-clinical characterization of [11C]R05013853 as a novel radiotracer for imaging of the glycine transporter type 1 by positron emission tomography. NeuroImage, 2013, 75, 291-300.	4.2	16
79	Dynamic PET-facilitated modeling and high-dose rifampin regimens for <i>Staphylococcus aureus</i> orthopedic implant–associated infections. Science Translational Medicine, 2021, 13, eabl6851.	12.4	16
80	¹⁸ F-XTRA PET for Enhanced Imaging of the Extrathalamic α4β2 Nicotinic Acetylcholine Receptor. Journal of Nuclear Medicine, 2018, 59, 1603-1608.	5.0	15
81	Osteopontin/secreted phosphoprotein-1 behaves as a molecular brake regulating the neuroinflammatory response to chronic viral infection. Journal of Neuroinflammation, 2020, 17, 273.	7.2	14
82	Synthesis of a Radiotracer for Studying k-Subtype Opiate Receptors: N-[11C-methyl]-N-(trans-2-pyrrolidinyl-cyclohexyl)-3,4-dichlorophenylacetamide ([11C](±)U-50488H). Journal of Labelled Compounds and Radiopharmaceuticals, 1992, 31, 81-89.	1.0	12
83	P4â€185: First inâ€human PET study of 3 novel tau radiopharmaceuticals: [¹¹ C]RO6924963, [¹¹ C]RO6931643, and [¹⁸ F]RO6958948. Alzheimer's and Dementia, 2015, 11, P850.	0.8	12
84	Effect of STN DBS on vesicular monoamine transporter 2 and glucose metabolism in Parkinson's disease. Parkinsonism and Related Disorders, 2019, 64, 235-241.	2.2	12
85	Brown Adipose Tissue Response Dynamics: In Vivo Insights with the Voltage Sensor 18F-Fluorobenzyl Triphenyl Phosphonium. PLoS ONE, 2015, 10, e0129627.	2.5	12
86	Effects of Vasopressin on Blood-Brain Transfer of Methionine in Dogs. Journal of Neurochemistry, 1992, 59, 1421-1429.	3.9	11
87	Synthesis of N1′-([18F]fluoroethyl)naltrindole ([18F]FEtNTI): a radioligand for positron emission tomographic studies of delta opioid receptors. Journal of Labelled Compounds and Radiopharmaceuticals, 1999, 42, 43-54.	1.0	11
88	Imaging α4β2 Nicotinic Acetylcholine Receptors (nAChRs) in Baboons with [18F]XTRA, a Radioligand with Improved Specific Binding in Extra-Thalamic Regions. Molecular Imaging and Biology, 2017, 19, 280-288.	2.6	11
89	¹¹ C-PABA as a PET Radiotracer for Functional Renal Imaging: Preclinical and First-in-Human Study. Journal of Nuclear Medicine, 2020, 61, 1665-1671.	5.0	11
90	11C-Para-aminobenzoic acid PET imaging of S. aureus and MRSA infection in preclinical models and humans. JCI Insight, 2022, 7, .	5.0	11

#	Article	IF	CITATIONS
91	Synthesis of 3-[(1-[11C]methyl-2(S)-pyrrolidinyl) methoxy]pyridine and 3-[(1-[11C]methyl-2(R)-pyrrolidinyl) methoxy]pyridine: Radioligands for in vivo studies of neuronal nicotinic acetylcholine receptors. Journal of Labelled Compounds and Radiopharmaceuticals, 1997, 39, 425-431.	1.0	10
92	Radiosynthesis and validation of [5â€cyanoâ€ <i>N</i> â€(4â€{4â€{ ¹¹ C]methylpiperazinâ€1â€yl)â€2â€(piperidinâ€1â€yl)phenyl) fu ([¹¹ C]CPPC), a PET radiotracer for imaging CSF1R, a microgliaâ€specific marker. Journal of Labelled Compounds and Radiopharmaceuticals, 2019, 62, 903-908.	ıranâ€2â€ 1.0	€earboxamide] 10
93	Molecular imaging of the serotonin transporter availability and occupancy by antidepressant treatment in late-life depression. Neuropharmacology, 2021, 194, 108447.	4.1	10
94	Cerebral Glucose Utilization in Polysubstance Abuse. Neuropsychopharmacology, 1995, 13, 21-31.	5.4	10
95	PET imaging of soluble epoxide hydrolase in non-human primate brain with [18F]FNDP. EJNMMI Research, 2020, 10, 67.	2.5	10
96	Effect of tracer metabolism on PET measurement of [11C]pyrilamine binding to histamine H1 receptors. Annals of Nuclear Medicine, 1999, 13, 101-107.	2.2	9
97	Synthesis of carbon-11 labeled methylcarbamates from [11C]-methylchloroformate. Journal of Labelled Compounds and Radiopharmaceuticals, 1995, 36, 365-371.	1.0	8
98	[125 l]Iodo-ASEM, a specific in vivo radioligand for α7-nAChR. Nuclear Medicine and Biology, 2015, 42, 488-493.	0.6	8
99	Development of a radioligand for imaging V 1a vasopressin receptors with PET. European Journal of Medicinal Chemistry, 2017, 139, 644-656.	5.5	8
100	An optimized radiosynthesis of [¹⁸ F]FNDP, a positron emission tomography radiotracer for imaging soluble epoxide hydrolase (sEH). Journal of Labelled Compounds and Radiopharmaceuticals, 2018, 61, 567-572.	1.0	8
101	The Relationship of Varenicline Agonism of α4β2 Nicotinic Acetylcholine Receptors and Nicotine-Induced Dopamine Release in Nicotine-Dependent Humans. Nicotine and Tobacco Research, 2020, 22, 892-899.	2.6	8
102	Synthesis and Evaluation of a New 18F-Labeled Radiotracer for Studying the GABAB Receptor in the Mouse Brain. ACS Chemical Neuroscience, 2018, 9, 1453-1461.	3.5	7
103	18F-labeled radiotracers for inÂvivo imaging of DREADD with positron emission tomography. European Journal of Medicinal Chemistry, 2021, 213, 113047.	5.5	7
104	In vivo studies of [1251]iodobenzamide and [11C]iodobenzamide: A ligand suitable for positron emission tomography imaging of cerebral D2 dopamine receptors. Synapse, 1992, 12, 236-241.	1.2	6
105	Radiosynthesis and validation of [<scp><i>Carboxy</i></scp> â€ ¹¹ C]4â€ <scp>A</scp> minobenzoic acid ([¹¹ <scp>C</scp>] <scp>PABA</scp>), a <scp>PET</scp> radiotracer for imaging bacterial infections. lournal of Labelled Compounds and Radiopharmaceuticals. 2019. 62. 28-33.	1.0	6
106	First-in-human neuroimaging of soluble epoxide hydrolase using [18F]FNDP PET. European Journal of Nuclear Medicine and Molecular Imaging, 2021, 48, 3122-3128.	6.4	6
107	Radiosynthesis of [5â€[¹¹ C]methanesulfonylâ€2â€{(<i>S</i>)â€2,2,2â€trifluoroâ€1â€methylâ€ethoxy)â€phenyl]â€ ([¹¹ C]RO5013853), a novel PET tracer for the glycine transporter type I (GlyT1). Journal of Labelled Compounds and Radiopharmaceuticals. 2011. 54. 702-707.	{5â€(tetr 1.0	ahydroâ€pyrai
108	Regional amyloid correlates of cognitive performance in ageing and mild cognitive impairment. Brain Communications, 2022, 4, fcac016.	3.3	5

#	Article	IF	CITATIONS
109	External monitoring of cerebral nicotinic acetylcholine receptors in living mice. Synapse, 1997, 27, 378-380.	1.2	4
110	A side-by-side evaluation of [18F]FDOPA enantiomers for non-invasive detection of neuroendocrine tumors by positron emission tomography. Oncotarget, 2019, 10, 5731-5744.	1.8	3
111	Assessing neuroreceptor occupancy by continuous infusion of carbon-11 labeled radioligands. European Journal of Nuclear Medicine and Molecular Imaging, 1996, 23, 141-144.	2.1	2
112	Synthesis of 3-[(1-[11C]methyl-2(S)-pyrrolidinyl) methoxy]pyridine and 3-[(1-[11C]methyl-2(R)-pyrrolidinyl) methoxy]pyridine: Radioligands for in vivo studies of neuronal nicotinic acetylcholine receptors. Journal of Labelled Compounds and Radiopharmaceuticals, 1997, 39, 425-431.	1.0	2
113	Characterization of dose dependent norepinephrine transporter blockade by atomoxetine in human brain using 11C MeNER PET. Journal of Cerebral Blood Flow and Metabolism, 2005, 25, S599-S599.	4.3	2
114	PET/CT imaging of CSF1R in a mouse model of tuberculosis. European Journal of Nuclear Medicine and Molecular Imaging, 2022, 49, 4088-4096.	6.4	1
115	Radiosynthesis of the α4β2 nicotinic acetylcholine receptor ligand: 5-((1-[11C]-methyl-2-(S)-pyrrolidinyl)methoxy)-2-chloro-3-((E)-2-(2-fluoropyridin-4-yl)vinyl)pyridine. Journal of Labelled Compounds and Radiopharmaceuticals, 2006, 49, 459-462.	1.0	0
116	Bengt Långström-personal recollections of the gentle giant of short-lived radiotracers. Journal of Labelled Compounds and Radiopharmaceuticals, 2015, 58, 49-50.	1.0	0